Vibration-based unsupervised detection of common faults in rotating machinery under varying operating speeds

Dimitrios M. Bourdalos & John S. Sakellariou
Stochastic Mechanical Systems Automation (SMSA) Laboratory
Department of Mechanical Engineering and Aeronautics, University of Patras 26504 Patras, Greece
dimitrios.bourdalos@upnet.gr, sakj@mech.upatras.gr

Abstract

The detection of common incipient faults in rotating machinery operating under varying speeds is presently investigated via two unsupervised machine learning type methods using a limited number of vibration signals from a single sensor for their training. The first utilizes advanced Functional Pooled (FP) AutoRegression (AR) modelling for the explicit interpretation of the machinery healthy dynamics within the complete range of rotating speeds, while the second employs a cloud of typical AR models within a Multiple Model framework. The methods' performance is systematically assessed and compared based on hundreds of experiments with the healthy and faulty machinery that consists of two electric motors coupled via a claw clutch and operate under 75 different rotating speeds. Three types of incipient faults are separately incorporated, a slight unbalance, minor wear at the base of a single claw clutch (coupler) tooth, and mechanical looseness at one of the four main mounting bolts of the machinery. The results indicate the clear superiority of the FP based method that achieves impressive detection of all considered faults even under rotating speeds for which it is not trained.

1 Introduction

Condition monitoring of rotating machinery has received major attention for many decades due to the involvement of drivetrains, gearboxes and so on in many engineering systems as for instance in wind turbines, vehicles, robotics and industrial infrastructures [1]. Great emphasis with numerous applications, has been given to *vibration-based* condition monitoring methods due to various advantages as it is their global nature, the wide variety of data acquisition and sensors of reasonable cost, their high effectiveness and so on [2]. Vibration-based fault detection relies on the fact that a potential fault causes changes in the machinery dynamics and this is reflected in the measured vibration signals. However, in most applications rotating machinery operates under *different conditions*, as it is the rotating speed and the load, which have significant effects on the vibration signals resembling with potential faults, especially if the latter are at an early stage. This renders the detection of incipient faults in rotating machinery a highly challenging problem necessitating robust methods that may separate the effects of the varying Operating Conditions (OCs) from those due to faults and eliminate false alarms in order to ensure reliable condition monitoring systems.

The varying OCs can be classified into *three categories* [3]. The first involves fully random fluctuations to the OCs of the rotating machinery as for instance is the case of wind ambient excitation to wind turbines [3, 4]. The second refers to cyclic variations to the OCs such as those encountered in bucket wheel excavators [5], while the third category, which is the most common, refers to the machinery operation under multiple levels of OCs that remain constant for a specific period of time, which is the focus of this study. Such OCs typically occur in industrial applications with different production phases, where both the load and speed of the machinery may vary multiple times according to the needs, as well as in transportation where the vehicles operate at different speeds and payload which are constant for certain segments of their route.

The vibration-based methods which focus on the detection of early stage faults under multiple levels of OCs may be classified into two broad families: The *Supervised* and the *Unsupervised*. *Supervised* detection methods address the problem using data from both the healthy and the faulty machinery for their training, while the *unsupervised* are exclusively based on data from the healthy machinery [6, p. 12].

The vast majority of applications in the pertinent literature are based on *supervised* methods utilizing typical features in time domain (e.g. Peak, RMS, Kurtosis, Crest factor) [7, 8, 9] or in frequency domain (e.g. Mean

Frequency) [7, 8] or in time-frequency domain. Time-frequency domain features are usually based on Short-Time Fourier Transform for the construction of vibration spectral images [10], Empirical Mode Decomposition for Intrinsic Mode Functions (IMFs) entropy determination [8, 11, 12] or Wavelet Packet Transformation for entropy determination of specific frequency bandwidth signals [8, 11]. Alternatively, more special features have been also employed using prior knowledge on the fault type of interest and its special effects on the vibration signal characteristics [7, 8]. The concept behind these methods resides in these special features' high sensitivity to faults and their insensitivity to the multiple operating conditions. Various of all the above features have been combined with machine learning classification algorithms such as Support Vector Machine (SVM) [9, 11] and k-Nearest Neighbor (k-NN) [7, 12] as well as with statistical distances [10] achieving the detection of incipient gear cracks [7, 8, 12] and rolling bearing defects [10, 11] under a limited number of different operating speeds or loads. Furthermore, *supervised* methods have been effectively employed for the detection of incipient gear and bearing defects under a limited number of rotating speeds and loads based on Convolutional Neural Networks [13, 14], Inception Networks [15], Deep Neural Networks [16, 17] or Adversarial networks [18, 19] using as inputs raw time-domain vibration signals [13, 15, 18] or their time-frequency representations [14, 16, 17, 19].

The most important drawback of the supervised fault detection methods lies in the fact that the methods' training necessitates data from *every* different operating condition (speed and/or load) of the machinery and *both* health states (healthy/faulty) which is impossible in most industrial applications. Combined with this, a significant number of experiments for the collection of a multitude of vibration signals (oftentimes collected via multiple sensors) is in most cases required for their training, as well as for the special features-based methods the effects of the considered fault on the signals vibration characteristics should be a-priori known.

On the other hand, the available *unsupervised* methods aim at the detection of faults under multiple operating conditions using initially filtering and denoising computationally demanding techniques, as it is the well-known Time Synchronous Averaging (TSA), for the removal of the repetitive signal which is related to a specific component (gear or bearing), provided that the component's characteristic repetitive frequency is accurately known. The processed signals are then used for the identification of distinct typical AutoRegressive (AR), Moving Average (MA) with eXogenous (ARMAX) input type models for the modelling of the healthy rotating machinery dynamics under the different operating conditions of interest. Then, fault detection is based on proper testing of the model residual characteristics (e.g. sample variance, kurtosis). Faults with however noticeable imprint in the time domain vibration signals, have been detected using ARMA or AR [20] models for a limited number of different loads. More recently, AR [21], ARX [22] or Vector AR (VAR) [23] models have been employed in this context for the detection of faults under a few different loads using multiple sensors on the machinery. Yet, the results from run-to-failure experiments resulting in a total crack and removal of a single or multiple gear teeth are presented, thus being unclear whether fault detection has been achieved at an incipient level of the fault. The key benefit of the *unsupervised* methods is the use of vibration data for their training collected exclusively from the healthy machinery under different operating conditions which is possible in almost all applications.

It is also worth stressing that the detection performance of *incipient faults* using either supervised or unsupervised methods have been thus far assessed under a *limited* number of different operating conditions, specifically loads (five at maximum), while fault detection within a wide range of speed levels is unexplored. Obviously, the study of both issues is important based on the fact that typically the operating conditions may significantly vary, as it is the case for an industrial rotating machinery used in a production line, while speed variation has significantly higher impact on the observed dynamics than load implying a more challenging fault detection problem.

The *goal* of this study is the examination of the potential for automated vibration-based detection of common incipient faults in a rotating machinery operating under many different levels of speed without any a-priori information about the considered faults, based on: (i) two unsupervised machine learning methods, (ii) a reasonable amount of signals from the healthy machinery for the methods' training (learning) phase and, (iii) a single accelerometer on the machinery. The first method, utilizes a single stochastic Functionally Pooled AutoRegressive (FP–AR) Model [24] with a scalar operating parameter corresponding to the rotating speed of the machinery for the interpretation of its healthy dynamics, while fault detection is based on nonlinear optimization and model residual whiteness hypothesis testing. The second method interprets the healthy dynamics using a cloud of conventional AR models within a Multiple Model framework [25] and the detection is achieved via a similarity distance metric. The questions posed in this study are:

- Is it possible to detect incipient faults with no effects on typical time domain characteristics in a rotating machinery that operates under multiple levels of speed using vibration signals from a single accelerometer?

- Is it possible to achieve a high True Positive Rate ($> 95\%$) for low ($\leq 5\%$) False Positive Rate (FPR) indicating correct fault detection with low false alarms for common faults using a single experiment, a limited number of signals and no information about the faults for the methods' training?

In addition, the methods' performance is systematically assessed based on hundreds of test cases with a rotating machinery that consists of two coupled (via a claw clutch) electric motors operating at 75 distinct speeds under healthy and faulty conditions. The latter include three different in type, yet common, incipient fault scenarios which are considered separately in the machinery. The first corresponds to slight unbalance, the second to minor wear at the base of a single claw clutch (coupler) tooth, and the third to mechanical looseness at one of the four drive motor mounting bolts. The results of the study are presented via scatter type plots of the fault detection characteristic quantities per method and Receiver Operating Characteristic (ROC) curves. Results from some first efforts on the problem have been presented in a recent conference paper of ours in [26].

2 The experimental set-up

2.1 The rotating machinery, the incipient fault scenarios and the vibration signals

The rotating machinery (Fig. 1 (a)) consists of two foot-mounted electric motors coupled via a claw clutch and operates under 75 distinct speeds in the range between 35 Hz (2094 rpm) and 49.8 Hz (2982 rpm) with a 0.2 Hz (12 rpm) step, selected through a typical variable frequency driver. Three common incipient fault scenarios of different type are separately implemented in the machinery: (i) limited unbalance induced by replacing the main coupler mounting bolt with a 3g heavier as shown in Fig. 1 (b), (ii) coupler wear corresponding to incipient wear at the base of a single spider tooth as shown in Fig. 1 (c) and, (iii) mechanical looseness implemented via torque reduction from 5 to 2.5 Nm to the drive-motor mounting Bolt A (Fig. 1 (a)).

The acquisition of the vibration signals which are used for the training and assessment of the machine learning methods is performed using a single uniaxial lightweight accelerometer mounted on the drive-motor

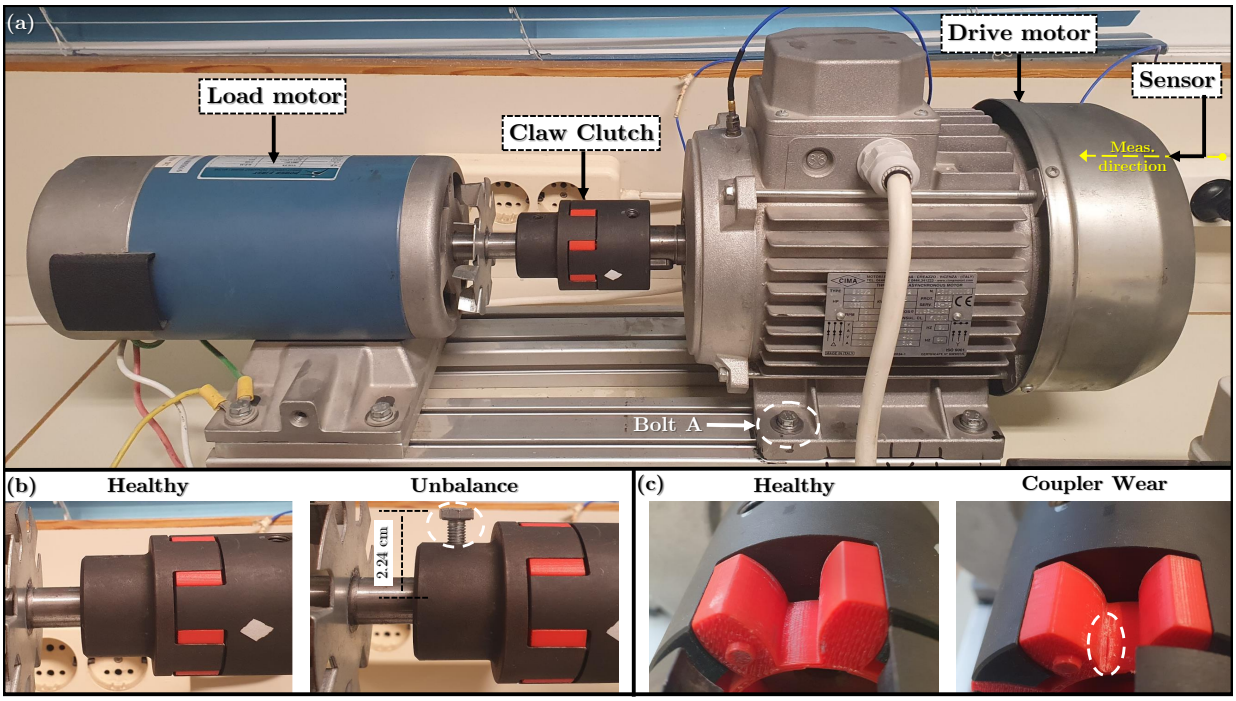

Figure 1: (a) Photo of the rotating machinery components including the location of the used sensor (accelerometer) and the Bolt A where the mechanical looseness is performed, (b) the unbalance fault scenario using a heavier coupler mounting bolt, (c) the coupler wear.

Table 1: Details on the vibration signals used for the training and assessment of the machine learning methods.

Machinery state	Rotating speed (Hz)	Mounting Tightening torque (Nm)	No. of signal segms. per speed	Total no. of signal segments
Training (learning) phase				
Healthy	$\{35, 35.4, \ldots, 49.8\}$ (step of 0.4 Hz)	5	1	38
Inspection phase				
Healthy	$\{35, 35.2, \ldots, 49.8\}$ (step of 0.2 Hz)	5	2*	187
Unbalance	——"——	5	2	150
Coupler wear	——"——	5	2	150
Mech. Looseness	——"——	2.5	2	150
Sampling frequency: $f_s = 1024$ Hz, Signal segment length: $N = 3500$ samples (3.42 s)				
Frequency bandwidth: $BW = [0 - 512]$ Hz				

*3 signal segments for the 37 rotating speeds not used in the training (learning) phase

as shown in Fig.1 (a) with a sample frequency of $f_s = 1024$ Hz via the following procedure: Initially, the machinery is at its healthy condition and the rotating speed is set to the minimum (of interest) speed of 35 Hz and the signal acquisition runs for 3.42 seconds. The rotating speed is instantly increased to the next level (35.2 Hz) with a step of 0.2 Hz, and the acquisition of a new vibration signal is performed. This procedure continues until the maximum rotating speed of interest (herein 49.8 Hz) is reached. This procedure is in this study repeated three times with the healthy machinery resulting thus in three distinct vibration signals each of 262 500 samples.

The same procedure is subsequently performed two times for each fault scenario and two vibration signals of the same length as above are obtained. 9 vibration signals of the same length are in total available after a respective number of experiments, three from the healthy machinery and two from each of the considered fault scenario. An indicative vibration signal from the healthy machinery as well as from each considered fault scenario is shown in Fig.2 (a).

Each of the acquired signals is divided into 75 segments, one for each rotating speed, resulting thus in a total of 675 (9×75) signal segments with each consisting of 3 500 samples. The training of the machine learning methods for fault detection is based on 38 signal segments from the first experiment with the healthy machinery corresponding to the 5.6% of the total data base signal segments, while the remaining 637 segments (94.4%) are exclusively used in the inspection phase for the methods assessment and comparison. All details on the vibration signals are included in Table 1.

2.2 Effects of the different operating speeds and incipient faults on the machinery

The effects of the different rotating speeds and the considered fault scenarios on the machinery are examined through the RMS values of the vibration signals in the time domain, as well as in the frequency domain using the signal segments Power Spectral Density (PSD). As mentioned previously, Fig.2 (a) depicts indicative vibration signals from the healthy and faulty machinery, Fig.2 (b) includes the rotating speed profile used in each experiment, and Fig. 2 (c) indicates the RMS values as obtained from each of the 75 vibration signal segments. Based on Figs.2 (a) and (c), it is evident that the effects of the coupler and the motor mounting faults to the RMS lies in the same range of values with those of the healthy machinery, indicating a highly challenging fault detection problem. The picture is similar for the effects due to the unbalance fault scenario, except for the speed range between 41.6 Hz and 47.2 Hz, where the unbalance leads to higher RMS values compared with the healthy machinery at the same speeds, indicating thus a potential fault. However, the unbalance to other operating speeds where the machinery may operate under normal conditions is not detectable via the RMS values resulting thus to its faster degradation.

In addition, the effects of the different rotating speeds on the healthy machinery dynamics and those due to the considered faults are presented in Fig. 3 through PSD Welch-based [27, p. 186] estimates (Hamming window length = 2048 samples, Overlap = 95%, frequency resolution: $\delta f = 0.5$ Hz). The challenge in the detection of the considered incipient faults is confirmed based on the fact that the effects of the different rotating

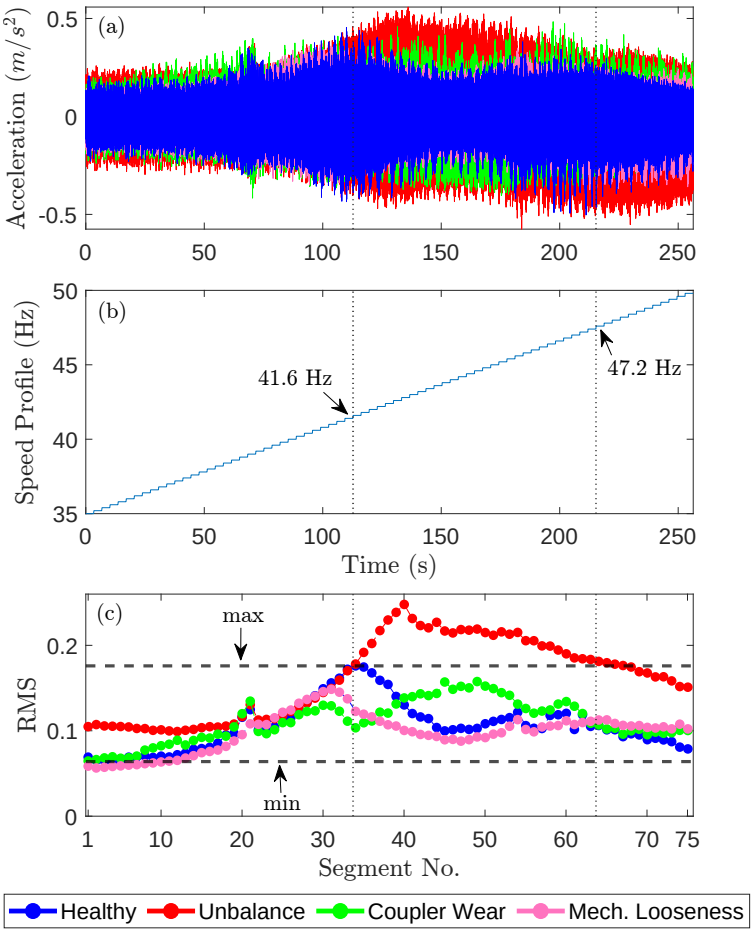

Figure 2: (a) Indicative vibration signals for each machinery health state (1 signal of 262 500 samples per state), (b) rotating speed profile per experiment (75 different speeds; step of 0.2 Hz), (c) RMS values per vibration signal segment (75 segments of 3 500 samples per health state). The RMS limits which are determined by the min and max RMS values among the 75 signal segments of the healthy machinery are indicated with black dashed lines.

speeds on the healthy dynamics mask those induced by the considered fault scenarios especially for the coupler wear and the mechanical looseness where the PSD envelopes almost coincide for the complete frequency bandwidth.

3 The unsupervised machine learning methods for fault detection

3.1 The Functionally Pooled (FP) model based method

Training (learning) phase: The cornerstone of this method is the representation of the healthy rotating machinery dynamics at any rotating speed within the range of interest using a single Functionally Pooled AR (FP–AR) model, which is estimated offline in this phase of the method, of the form [24]:

$$\begin{gathered} y_k[t] + \sum_{i=1}^{na} a_i(k) \cdot y_k[t-i] = e_k[t], \quad e_k[t] \sim \text{NID}(0, \sigma_e^2(k)) \text{ with } k \in R \\ a_i(k) = \sum_{j=1}^{p} a_{i,j} \cdot G_j(k) \end{gathered} \tag{1}$$

where $t = 1, \ldots, N$ designating discrete time, k rotating speed, na the AR model order, $e_k[t]$ model residual signal and NID $(\cdot,\cdot)$ Normally Independently Distributed with the indicated mean and variance. The AR parameters $a_i(k)$ are modelled as explicit functions of k using a p-dimensional functional subspace spanned by the mutually independent functions $G_1(k), \ldots, G_p(k)$, while the constants $a_{i,j}$ designate the corresponding AR

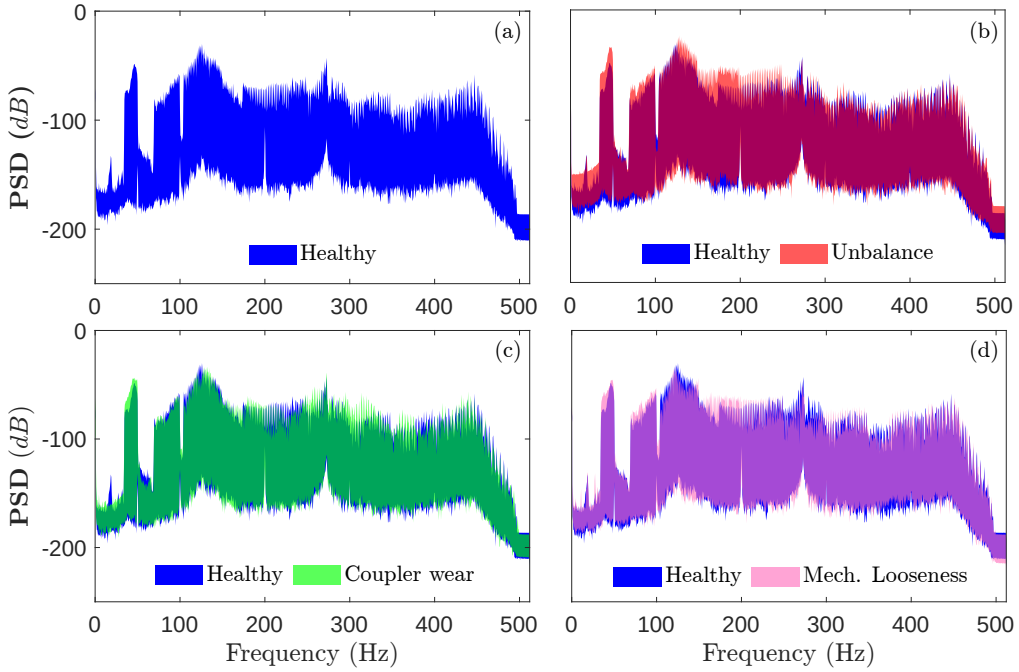

Figure 3: Envelopes of Welch-based PSD estimates constructed using the (38) vibration signal segments (3 500 samples each) of the training phase with the healthy machinery and signals from the same rotating speeds under the considered faults: (a) Healthy, (b) Healthy vs Unbalance, (c) Healthy vs Coupler Wear, (d) Healthy vs Mechanical Looseness.

projection coefficients. Model identification includes: (i) determination of the FP–AR model order na and its functional subspace dimensionality p for a given basis function family (e.g. polynomials Legendre, Chebyshev) using a Genetic Algorithm (GA) for the minimization of the Bayesian Information Criterion (BIC), (ii) model validation via testing of the obtained model residual signals whiteness hypothesis and, (iii) model estimation based on Ordinary Least Squares (OLS) with 'data pooling' [24] using n vibration signals from the healthy machinery operating under a sample of rotating speeds within the range of interest $[k_{min}, k_{max}]$.

Inspection (real time) phase: Once a vibration signal $y_u[t]$ is obtained from the rotating machinery under unknown health state and rotating speed k, the fault detection procedure is activated using the FP model of the previous phase. This is achieved by testing if the current machinery dynamics, as reflected by the $y_u[t]$, is represented by the FP–AR$(na)_p$ model of the previous phase that corresponds to the healthy machinery. To this end, $y_u[t]$ is driven through the FP–AR$(na)_p$ and a Nonlinear Least Squares (NLS) optimization algorithm for scalar variables implemented via golden search and parabolic interpolation is employed for the estimation of k that leads to the minimum residual sum of squares [28]:

$$\widehat{k} = \arg\min_{k} \sum_{t=1}^{N} e_u^2[t,k], \quad \widehat{\sigma}_e^2(\widehat{k}) = \frac{1}{N}\sum_{t=1}^{N} e_u^2[t,\widehat{k}] \tag{2}$$

with $e_u[t,\widehat{k}]$ designating the model residual signal under the unknown state that is obtained using $\widehat{k}$ in Equation 1. If the current dynamics originates from the healthy machinery then $e_u[t,\widehat{k}]$ should be a white (uncorrelated) signal which may be examined via any typical whiteness testing procedure; herein the Pena-Rodriguez D statistic which follows a standard normal distribution for a white sequence [28] is employed. If $e_u[t,\widehat{k}]$ is white this means that $y_u[t]$ originates from the healthy machinery operating under $\widehat{k}$ speed, otherwise the machinery is declared as faulty. It is noted that in case of a healthy declaration, an interval estimate of the current operating condition (herein rotating speed) is also provided to the user.

3.2 The Multiple Model based method

Training (learning) phase: The concept behind this method [25] is herein the representation of the healthy dynamics via multiple AutoRegressive models (MM-AR) of order na (not necessarily the same with the previous method), estimated using a number of n vibration signals with the machinery operating under a sample

of rotating speeds within the range of interest. Thus, a set $\mathbb{M}_o$, with 'o' indicating the 'healthy' state, of AR models using standard identification procedures [27, pp.81-83] is obtained with each model denoted as $M_{o,i}$ $(i = 1,\ldots,n)$.

Inspection (real time) phase: Once a signal $y_u[t]$ from the machinery under unknown health state and rotating speed is collected, an AR model M_u (subscript 'u' stands for unknown health state) of the same order *na* as those in $\mathbb{M}_o$ is estimated. If M_u, representing the current machinery dynamics, belongs to the MM representation $\mathbb{M}_o$, the machinery is declared as healthy otherwise as faulty. This is examined via the following decision-making mechanism that is based on a similarity distance metric Q:

$$Q := \min_i d(M_{o,i}, M_u), \quad \text{for } i = 1,\ldots,n \tag{3}$$

with $d(M_{o,i}, M_u)$ indicating the Mahalanobis distance [25] between two individual models. Then, based on a user specified threshold L_{lim} determined in the learning phase, fault detection is achieved as follows:

$$\begin{aligned} Q \leq L_{lim} &\rightarrow \text{Healthy Machinery} \\ \text{Else} \quad &\rightarrow \text{Faulty Machinery} \end{aligned} \tag{4}$$

4 Experimental Results

Training (learning) phase: $n = 38$ acceleration signals corresponding to a sample of 38 different rotating speeds (35 - 49.8 Hz with a step of 0.4 Hz) as shown in Table 1 are used for the identification of an FP–AR$(140)_{18}$ model with order $na = 140$ and functional subspace consisting of $p = 18$ Shifted Legendre polynomials (also see Table 2). This model represents the rotating machinery healthy dynamics within the continuous range $[35, 49.8]$ Hz of rotating speeds. Based on the same set of vibration signals, 38 conventional AR(140) models are also obtained. Estimation details for both models are provided in Table 2.

Table 2: Details on the model estimation per method.

Method	Model	Samples Per Parameter	Condition Number	BIC
FP model based	*FP–AR$(140)_{18}$	52.78	$1.16 \cdot 10^7$	-36.41
MM-AR based	AR(140)	25	$1.15 \cdot 10^5$	-7.78
$^*G_j : j = 3,4,5,10,12,14,15,17,21,26,27,28,30,31,33,35,36,37$				

Inspection (real time) phase: 187 signals from the healthy machinery and 150 from each fault scenario with the machinery operating under 75 rotating speeds (not only those used in the training phase, see Table 1) within the range of interest (35 - 49.8 Hz) are used in this phase for the methods' fault detection performance assessment. It is noted that each of the available signal segments (Table 1) corresponds to a single test case, while the machinery health state and the rotating speed are considered as completely unknown in each test case. The D statistic of the FP–AR method and the Q metric for all considered test cases (637) are presented in Fig. 4 via scatter type plots and Receiver Operating Characteristic (ROC) curves. The H_1 set of test cases correspond to measurements (different signals) under the 38 rotating speeds which are also used in the methods' training, while the H_2 to the rest 37 available speeds (see Table 1).

Based on the values of the Pena-Rodriguez D statistic (Fig. 4 (a)) of the FP–AR based method, it is evident that those of the H_1 and H_2 test cases corresponding to the healthy machinery are almost fully separated from those obtained from the considered fault scenarios indicating remarkable fault detection performance even for the test cases with rotating speed not included in the method's training. These results are also validated by the corresponding ROC curves in Fig. 4 (b) which indicate 100% TPR (correct detection) with 0% FPR (false alarms) for the unbalance fault scenario, and 97% with 5% FPR for the coupler wear and mechanical looseness scenarios.

On the other hand, the fault detection results based on the values of the Q similarity metric of the MM–AR method (Figs. 4 (c)) indicate the method's poor performance as there is significant overlap among the values corresponding to the healthy and faulty machinery, which is also confirmed by the corresponding ROC curves in Fig. 4 (c)) that significantly deviates from the point (0,1) of flawless performance. More specifically, although only a few values from the H_1 set of test cases lie in the range of Q values corresponding to faults, there is no

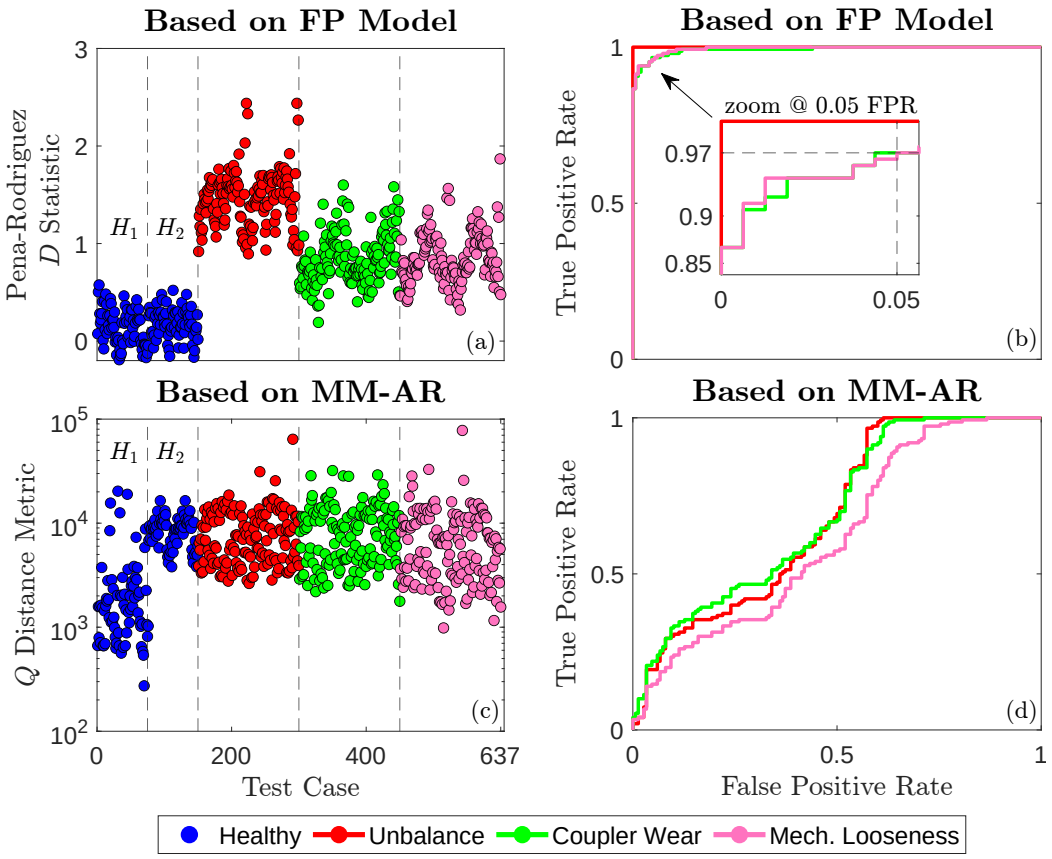

Figure 4: Fault detection results: (a) Pena-Rodriguez D statistic of the FP based method, (c) Q distance metric of the MM–AR based method and (b), (d) corresponding ROC curves. [637 inspection cases including 75 rotating speeds per method; the H_1 test cases correspond to the healthy machinery operating under speeds used in the methods' training, while H_2 to completely unknown speeds].

value from the H_2 set out of this range. This pinpoints the limitation of the MM–AR based method to operate in a different range of rotating speeds other than that it is trained. This happens as the MM–AR based method approximates the healthy dynamics using distinct AR models in contrast to the FP–AR based method where the *continuous* healthy dynamics is modelled via a single FP–AR model. It is worth mentioning that for the test cases where no fault is detected, the FP based method provides accurate estimation of the machinery unknown rotating speed achieving a mean error of 0.005 Hz ($\pm$ 0.042) based on the results of the 187 test cases of the inspection phase with the healthy machinery.

5 Concluding Remarks

The detection of three common incipient faults (unbalance, worn coupler, mechanical looseness) in a rotating machinery operating under 75 distinct speeds has been explored in this study via two unsupervised vibration-based machine learning methods, the FP–AR based and the MM–AR based ones. Their assessment has been performed via 637 test cases incorporating the healthy and faulty machinery. The main conclusions from the study which also answer to the main questions posed in the introduction follow:

(i) All considered incipient faults have been detected under any operating speed within the range of interest, although their effects on the signals RMS values are similar with those caused by the different rotating speeds to the signals of the healthy machinery. Only the unbalance fault indicated higher RMS values in a limited range of rotating speeds between 41.6 Hz and 47.2 Hz.

(ii) The FP–AR based method achieved remarkable fault detection results with 100% TPR and 0% FPR for the unbalance fault scenario and 97% TPR with 5% FPR for the worn coupler and mechanical looseness fault scenarios using 38 vibration signals (5.6% of the whole data base) obtained from a single experiment with

the healthy machinery and no information about the considered faults. On the other hand the performance of the MM–AR method was inadequate.

Acknowledgements

This research work was supported by the Hellenic Foundation for Research and Innovation (HFRI) under the 4th Call for HFRI PhD Fellowships (Fellowship Number 10820).

References

[1] J. Chen, C. Lin, D. Peng, and H. Ge, *Fault Diagnosis of Rotating Machinery: A Review and Bibliometric Analysis*, IEEE Access 8, 2020, pp. 224985-225003.

[2] K. Feng, J.C. Ji, Q. Ni, and M. Beer, *A review of vibration-based gear wear monitoring and prediction techniques*, Mechanical Systems and Signal Processing 182, 2023, p. 109605.

[3] Y. Chen, S. Schmidt, P. S. Heyns, and M.J. Zuo, *A time series model-based method for gear tooth crack detection and severity assessment under random speed variation*, Mechanical Systems and Signal Processing 156, 2021, p. 107605.

[4] Y. Chen and M.J. Zuo, *A sparse multivariate time series model-based fault detection method for gearboxes under variable speed condition*, Mechanical Systems and Signal Processing 167, 2022, p. 1008539.

[5] W. Bartelmus and R. Zimroz, *A new feature for monitoring the condition of gearboxes in non-stationary operating conditions*, Mechanical Systems and Signal Processing 23(5), 2009, pp. 1528-1534.

[6] C.R. Farrar, and K. Worden, *Structural Health Monitoring: A Machine Learning Perspective*, John Wiley & Sons, 2012.

[7] Y. Lei and M.J. Zuo, *Gear crack level identification based on weighted K nearest neighbor classification algorithm*, Mechanical Systems and Signal Processing 23(5), 2009, pp. 1535-1547.

[8] Y. Lei, M.J. Zuo, Z. He, and Y. Zi, *A multidimensional hybrid intelligent method for gear fault diagnosis*, Expert Systems with Applications 37(2), 2010, pp. 1419-1430.

[9] J. Xie, L. Zhang, L. Duan, and J. Wang, *On cross-domain feature fusion in gearbox fault diagnosis under various operating conditions based on Transfer Component Analysis*, IEEE International Conference on Prognostics and Health Management (ICPHM), 2016, pp. 1-6.

[10] L. Ciabattoni, F. Ferracuti, A. Freddi, and A. Monteriu, *Statistical Spectral Analysis for Fault Diagnosis of Rotating Machines*, IEEE Transactions on Industrial Electronics, 2017, pp. 1-1.

[11] A. Tabrizi, L. Garibaldi, A. Fasana, and S. Marchesiello, *Early damage detection of roller bearings using wavelet packet decomposition, ensemble empirical mode decomposition and support vector machine*, Meccanica 50(3), 2015, pp. 865-874.

[12] D. Wang, *K-nearest neighbors based methods for identification of different gear crack levels under different motor speeds and loads: Revisited*, Mechanical Systems and Signal Processing 70-71, 2016, pp. 201-208.

[13] W. Zhang, C. Li, G. Peng, Y. Chen, and Z. Zhang, *A deep convolutional neural network with new training methods for bearing fault diagnosis under noisy environment and different working load*, Mechanical Systems and Signal Processing 100, 2018, pp. 439-453.

[14] S. Guo, T. Yang, H. Hua, and J. Cao, *Coupling fault diagnosis of wind turbine gearbox based on multitask parallel convolutional neural networks with overall information*, Renewable Energy 178, 2021, pp. 639-650.

[15] X. Li, X. Kong, J. Zhang, Z. Hu, and C. Shi, *A study on fault diagnosis of bearing pitting under different speed condition based on an improved inception capsule network*, Measurement 181, 2021, p. 109656.

[16] W. Lu, B. Liang, Y. Cheng, D. Meng, J. Yang, and T. Zhang, *Deep Model Based Domain Adaptation for Fault Diagnosis*, IEEE Transactions on Industrial Electronics 64(3), 2017, pp. 2296-2305.

[17] W. Xu, L. Jing, J. Tan, and L. Dou, *A Multimodel Decision Fusion Method Based on DCNN-IDST for Fault Diagnosis of Rolling Bearing*, Shock and Vibration, 2020, p. 8856818.

[18] M. Zhang, D.Wang, W. Lu, J. Yang, Z. Li, and B. Liang, *A Deep Transfer Model With Wasserstein Distance Guided Multi-Adversarial Networks for Bearing Fault Diagnosis Under Different Working Conditions*, IEEE Access 7, 2019, pp. 65303-65318.

[19] M. Zhang, W. Lu, J. Yang, D. Wang, and L. Bin, *Domain Adaptation with Multilayer Adversarial Learning for Fault Diagnosis of Gearbox under Multiple Operating Conditions*, Prognostics and System Health Management Conference (PHM-Qingdao), 2019, pp. 1-6.

[20] W. Wang, and A.K. Wong, *Autoregressive model-based gear fault diagnosis*, Journal of Vibration and Acoustics 124, 2002, pp. 172-179.

[21] Y. Zhan, and C.K. Mechefske, *Robust detection of gearbox deterioration using compromised autoregressive modeling and Kolmogorov-Smirnov test statistic. Part II: Experiment and application*, Mechanical Systems and Signal Processing 21(5), 2007, pp. 1983-2011.

[22] M. Yang, and V. Makis, *ARX model-based gearbox fault detection and localization under varying load conditions*, Journal of Sound and Vibration 329(24), 2010, pp. 5209-5221.

[23] C. Lin, and V. Makis, *Application of Vector Time Series Modeling and T-squared Control Chart to Detect Early Gearbox Deterioration*, International Journal of Performability Engineering 10(1), 2014, p. 105.

[24] J.S. Sakellariou, and S.D. Fassois, *Functionally Pooled models for the global identification of stochastic systems under different pseudo-static operating conditions*, Mechanical Systems and Signal Processing 72-73, 2016, pp. 785-807

[25] K.J. Vamvoudakis-Stefanou J.S. Sakellariou, and S.D. Fassois, *Vibration-based damage detection for a population of nominally identical structures: Unsupervised Multiple Model (MM) statistical time series type methods*, Mechanical Systems and Signal Processing 111, 2018, pp. 149-171.

[26] D.M.Bourdalos, I.A.Iliopoulos, and J.S.Sakellariou, *On the Detection of Incipient Faults in Rotating Machinery Under Different Operating Speeds Using Unsupervised Vibration-Based Statistical Time Series Methods*, Lecture Notes in Civil Engineering 254 LNCE, 2023, pp. 287-296.

[27] L. Ljung, *System Identification: Theory for the user*, 2nd edn. Prentice-Hall, New Jersey (US), 1999.

[28] T.C.I. Aravanis, J.S. Sakellariou, and S.D. Fassois, *A stochastic Functional Model based method for random vibration based robust fault detection under variable non-mameasurable operating conditions with application to railway vehicle suspensions*, Journal of Sound and Vibration 466, 2020, p. 115006.